Influence of Heat Input on Mechanical Properties and Microstructure of Austenitic 202 grade Stainless Steel Weldments

APURV CHOUBEY
Assistant Professor
Symbiosis Institute of Technology (SIT)
Symbiosis International University (SIU)
Lavale, Pune-412 115, Maharashtra State
INDIA
apurv.choubey@sitpune.edu.in http://www.sitpune.edu.in

VIJAYKUMAR S. JATTI
Assistant Professor
Symbiosis Institute of Technology (SIT)
Symbiosis International University (SIU)
Lavale, Pune-412 115, Maharashtra State
INDIA
vijaykumar.jatti@sitpune.edu.in http://www.sitpune.edu.in

Abstract: - Present research work investigates the effect of heat input (controlled by welding current, welding voltage and welding speed) on tensile strength, micro-hardness and microstructure of austenitic 202 grade stainless steel weldments produced by shielded metal arc welding (SMAW). The base material used in the present investigation was Cr-Mn SS and 308L SS solid electrode was used as the filler material. From the experimental results it was found that the increase in heat input affects the micro-constituents of base metal, and heat affected zone (HAZ). Tensile strength decreases with increase in heat input and from scanning electron microscopy of tensile test fractured surfaces exhibited ductile & brittle failure. From micro hardness data values it was observed that hardness of material increases with increase in heat input in weld pool and decreases in HAZ zone. Optical microscopy shows that smaller dendrite sizes and lesser inter-dendritic spacing were observed in the fusion zone at low heat input. And long dendrite sizes and large inter-dendritic spacing were observed in the fusion zone of the joint welded at high heat input. Further it was observed from the optical micrographs that the extent of grain coarsening in the HAZ increases with increase in heat input.

Key-Words: - Austenitic stainless steel, Heat affected zone, Micro-hardness, Shielded metal arc welding, Ductile facture, Ultimate tensile strength.

1 Introduction

Stainless steel is classified based on crystalline structure into three types viz. austenitic, ferritic and martensitic. Ferritic steels have a body-centered cubic (BCC) crystal structure. They usually have low nickel content and cannot be hardened by heat treatment. Martensitic steels are those that can be hardened by heat treatment. Austenitic steels have austenite as their primary phase with face centered cubic crystal. As these alloys constitutes single phase, they can be strengthened by work hardening or solid solution alloying. They find application in both mild and severe corrosive condition due to presence of chromium in austenitic stainless steel. They are also used at temperatures that range from cryogenic temperatures, where they exhibit high toughness, to elevated temperatures of nearly 600°C where they exhibit good oxidation resistance. Because the austenitic material is nonmagnetic, they are sometimes used in application where magnetic materials are not acceptable. The austenitic stainless steel family is divided into two basic categories viz. 300-series and 200-series stainless steel. Austenitic stainless steels (which contain 18% Cr–8% Ni) are engineering materials widely used in many branches of industry, especially in the food and beverage manufacturing and processing sector, due to their attractive combination of good mechanical properties, formability, and corrosion resistance.

Their corrosion resistance is afforded by a thin Cr_2O_3 surface film (typically 1–3 nm thick), known as passive film, which has self-healing capability in a wide variety of environments (Sedriks and Olsson et al.). Viano et al. investigated the effect of heat input and travel speed on microstructural characteristics and mechanical properties of welds in 20 mm thickness high strength low alloy steel HSLA 80, of Australian manufacture. They found that as the heat input is increased, the cooling rate decreased resulting in a larger cellular dendritic cell spacing, decreased acicular ferrite content, and coarser acicular ferrite laths. The effect of travel speed on delta ferrite cell spacing and prior austenite grain size was found to be co-dependent on the heat input and the thermal profile resulting from multiple electrodes welding. Prasad and Dwivedi investigated the influence of the submerged arc welding (SAW) process parameters on the microstructure, hardness, and toughness of HSLA steel weld joints. Results showed that the increase in heat input coarsens the grain structure both in the weld metal and heat affected zone (HAZ). The hardness has been found to vary from the weld centre line to base metal and peak hardness was found in the HAZ. Prasad et al. describes the effect of heat input on the microstructure and tensile properties of high strength low alloy steel weldments produced by submerged arc welding. Results showed that the increase in the heat input affects the proportions of different micro-constituents both in the weld metal and heat affected zone. It is observed that the tensile strength (UTS, YS) decreases with increase in heat input and scanning electron microscopy of tensile test fractured surfaces usually exhibited ductile failure.

Viano et al. showed an micro-structural analysis and mechanical properties of welds in 20 mm thickness high strength low alloy steel HSLA 80 and specimens were prepared using the double tandem (four wire) submerged arc welding process in which both heat input and travel speed were varied. The inclusion size distribution was determined for selected welds and showed that heat input had a major effect. Karthik et al. studied the weldability properties of the shielded metal arc welded and welded and tungsten inert gas welded austenitic 304 stainless. Both the process showed the tensile strength below the base metal value but the TIG welding better fracture strength than SMAW.

Sathiya et al. studied the bead-on -plate welds on AISI 904 L super austenitic stainless steel sheets using gas metal arc welding process. From the experimental results, the gray relational analysis is applied to optimize the input parameters simultaneously considering multiple output variables. In order to understand the micro-structural changes occurring in the weld zone is investigated through the optical microscopy. The hardness measurements were taken across the fusion zone. Kianersi et al. optimized welding parameters namely welding current and time in resistance spot welding (RSW) of the austenitic stainless steel sheets grade AISI 316L. Then the effect of optimum welding parameters on the resistance spot welding properties and microstructure of AISI 316L austenitic stainless steel sheets has been investigated. Aim of this study is to evaluate the effect of heat input on tensile strength, micro-hardness and microstructure of austenitic 202 grade stainless steel weldments produced by shielded metal arc welding.

2 Material and Methods

To study the influence of heat input on microstructure and mechanical properties of 202 grade stainless steel work material shielded metal arc welding process was employed. The base material used in the present investigation was in the form of 202 SS plates of sizes 150 mm X 75 mm X 3mm which were cut using wire-cut electrical discharge machine from a rolled sheet and the filler was “AWS E308L-16” solid electrode of 3.15 mm diameter. Table 1 shows the chemical composition of the base and the filler used.

Table1 Chemical composition

Elements	Base material (202 SS)	Filler material (AWS E308L)
Cr	13.34	18.00
Ni	0.2087	9.00
C	0.27	0.04
Mn	9.84	0.80
Si	0.460	0.90
S	0.0105	0.03
P	0.0693	0.04

In the present work double V-groove design was used so that welding could be accomplished ensuring full penetration. Before welding all the edges were thoroughly cleaned in order to avoid any source of contamination like rust, scale, dust, oil, moisture that could creep into the weld metal and later on could result possibly into a weld defect. Bead-on-plate SMAW was performed along the

centre line of solution annealed plates using electrode "AWS E308L-16" of diameter 3.15 mm.
The samples were denoted by A, B, C as shown in Fig. 1. Sample A of (75 A, 100 A, 125 A) were then ethched chemically in order to see the penetration macroscopically as well as to take optical microstructures of welded area. Sample B of (75 A, 100 A, 125 A) were polished at various grit papers and after cloth polishing micro-hardness were performed perpendicularly along weld pool, HAZ region and base metal. Sample C of (75 A, 100 A, 125 A) were used for tensile testing and its fractography.

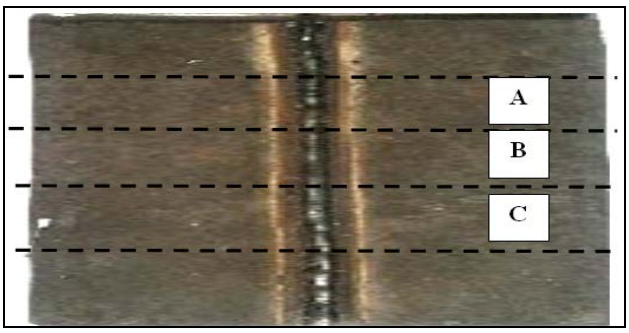

Fig.1 Bead-on-plate SMAW

After tacking the plates together the weld pass was given using SMAW process with welding conditions as mentioned in Table 2. Although SMAW process was used in the manual mode, still utmost care was taken during recording of the arc on time so as to facilitate calculations of heat input. It is worth mentioning here that the best welding practice available in the fabrication industry was used in the present work. It is a well established fact that among all the welding variables in arc welding processes welding current is the most influential variable since it affects the current density and thus the melting rate of the filler as well as the base material. A rest time of 30 seconds was allowed after every subsequent pass.
Heat input was calculated according to equation 1:

$$H = \frac{\eta * V * I}{v} \quad (1)$$

where, H= heat input in KJ/mm, η= efficiency = 0.75 for SMAW, V= voltage in volts, I= current in amperes, v= welding speed in mm/sec.

So in accordance with this fundamental fact three different heat input combinations corresponding to different welding currents i.e. 75 A (low heat input), 100 A (medium heat input) and 125 A (high heat input) combinations were selected for the present study. The reason for using these specific welding current values was twofold firstly, this spectrum of heat input combinations results in arc energies which are sufficient to cause adequate fusion of the base and weld metal selected for the present study and secondly, a step increase of 25 A was anticipated to be sufficient enough to cause a direct and significant influence on the microstructure and tensile properties of the welded joints. During and after welding the joints were visually inspected for their quality and it was ensured that all weld beads possessed good geometrical consistency and were free from visible defects like surface porosity, blow holes etc. Figure 2 shows the plates in the as welded condition using different heat inputs.

Table 2 Welding process parameters

Voltage (V)	Current (A)	Welding Speed (mm/sec)	Heat Input (KJ/mm)
35	75	2.50	0.787
35	100	2.50	1.050
35	125	2.50	1.312

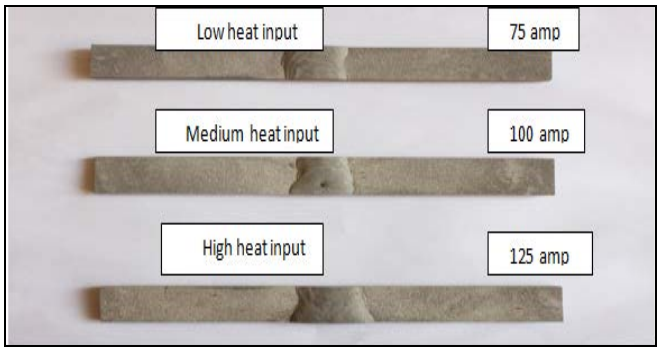

Fig.2 Welded samples at different heat inputs

In order to observe the micro-structural changes that take place during welding, corresponding to each heat input combination; specimens were machined out from the weld pads. After polishing and macro etching the cross sections of the joints were captured with the help of image analysis software coupled with a stereo zoom microscope at a magnification of 100X to facilitate measuring of the details like cross sectional areas of the fusion zone and HAZ. Standard polishing procedures were used for general micro-structural observations. Microstructures of different zones of interest like weld metal, HAZ and fusion boundary under different heat input combinations were viewed and captured with an

optical microscope (Zeiss Axiolab) coupled with an image analyzing software. The tensile specimen had a gauge length of 50 mm and they were fractured in an Instron machine as shown in Figure 3 with a cross head speed of 10 mm/min. During fractography the fractured ends of the tensile tested specimens were analyzed using scanning electron microscopy (SEM) to assess the nature of the fracture mode. The fractured surfaces of the tensile specimen were studied using JOEL; JSM Model 5900 LV SEM. All samples were examined at an accelerating voltage of 20 KV. The sampling of machined specimens at different heat input conditions were used measuring micro-hardness of different zones of the weldments. Vickers "s micrc hardness testing machine with a load of 300 gms was used in this study.

Fig.3 Tensile test setup

3 Results and Discussions

This section illustrates the results obtained from the optical micrograph and tensile test. The microstructures of fusion boundary and heat affected zone produced during welding at varying heat input conditions are shown in figure 4a, 4b and 4c, which also shows the welded region, narrow fusion zone and initiation of HAZ.

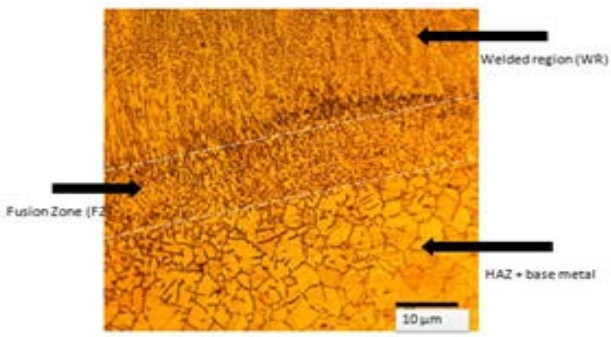

Fig.4 a) Optical micrograph at low heat input

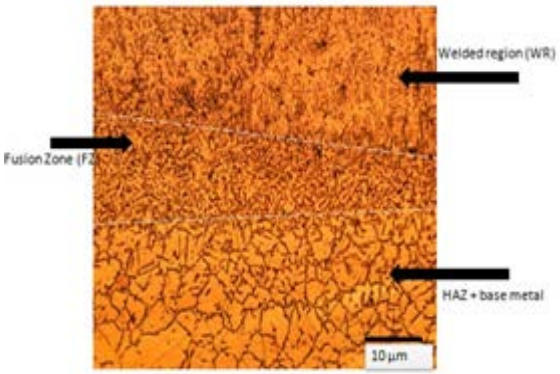

Fig.4 b) Optical micrograph at medium heat input

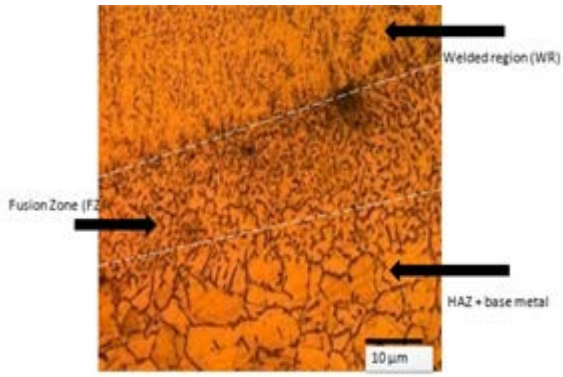

Fig.4 c) Optical micrograph at high heat input

3.1 Micro-hardness of austenitic stainless steel

Micro hardness measurements were taken in the transverse direction i.e. perpendicular to the base plate surface plate surface and the same are shown in figure 5a and 5b. Figure also shows that the micro hardness near the top of the weld bead surface is high and as the centre of the fusion/weld zone is approached by the indentor it gradually reduces, which is due to the fact that cooling rate is relatively higher at the top of the weld bead surface than at the centre of the weld metal. From table 3, it is observed that as the indentor traverses outwards (parallel to the base plate surface) from the centre of the weld/fusion zone towards the fusion boundary, micro hardness increases from 207.3 VHN for low heat input, 194 VHN for medium heat and 181 VHN for high heat input welded joint around HAZ region.

Table 3 Micro hardness values at different weld regions

Weld region	Low heat input	Medium heat input	High heat input
Weld pool	207.30	194.37	181.46
HAZ	229.10	208.42	193.76
Base metal	242.93	242.93	242.93

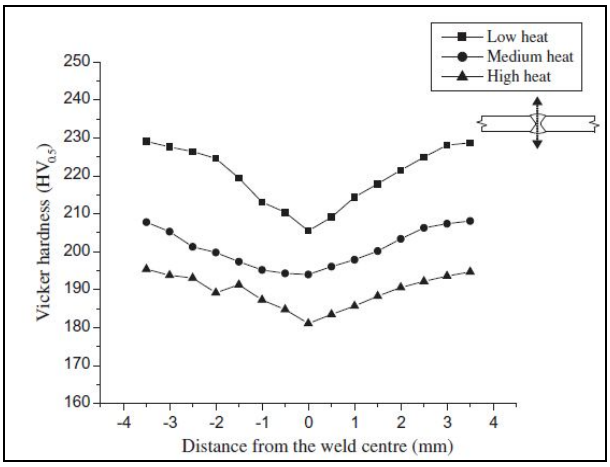

Fig.5 a) Micro hardness at different zones of the weldments at different heat inputs

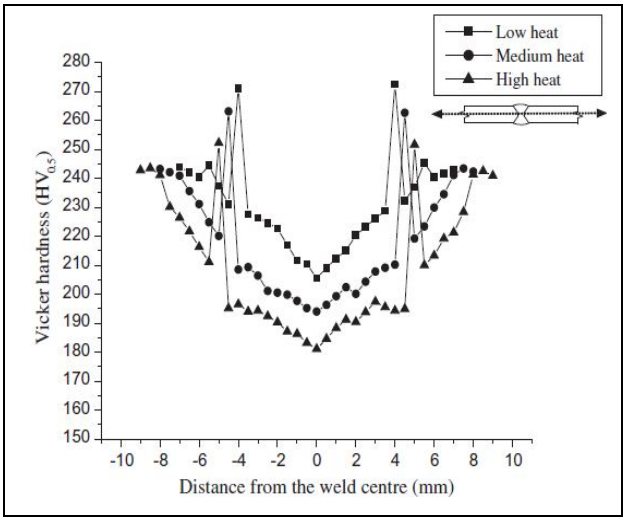

Fig.5 b) Micro hardness at different points of the weldments at different heat inputs

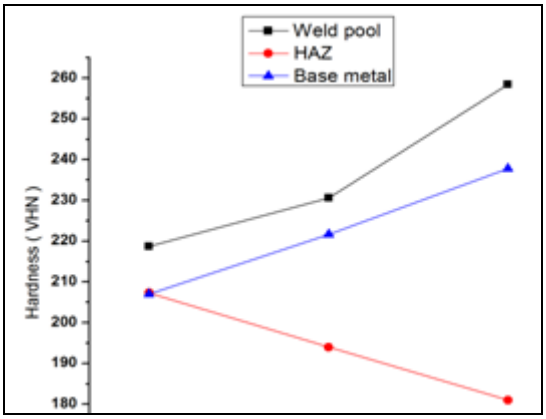

Fig.6 Micro hardness along weld pool, HAZ and base metal at different heat input

Fusion boundary or transition zone encountered while traversing in this direction is indicated by a steep rise in the micro hardness with value of 218.7 VHN, 230.6 VHN and 258.4 VHN respectively for low, medium and high heat input as shown in figure 6. High hardness as possessed by the fusion boundary zone (FBZ) in all the joints can be attributed to the presence of partially unmelted grains at the fusion boundary which are partially adopted as nuclei by the new precipitating phase of the weld metal during the solidification stage. After reaching this peak value micro hardness shows a decreasing trend in the HAZ. In all the joints, HAZ area adjacent to the fusion boundary was coarse grained HAZ (CGHAZ) which possessed low hardness whereas the HAZ area adjacent to the base metal was fine grained HAZ (FGHAZ) which possessed high hardness. The reason for this trend of micro hardness in the HAZ of all the joints is that the area adjacent to the weld/fusion zone experiences relatively slow cooling rate and hence has coarse grained microstructure, whereas the area adjoining the base metal undergoes high cooling rate due to steeper thermal gradients and consequently has fine grained microstructure. This is evident from the trend depicted by the micro hardness profile within the HAZ of each of these joints. In general it is observed from these micro hardness studies that hardness follows an increasing trend in the order of weld metal, HAZ, unaffected base metal and fusion boundary for all the joints made at different heat inputs. It is also observed that there is significant grain coarsening in the HAZs of all the joints. Further it is observed from the optical micrographs shown that the extent of grain coarsening in the HAZ increases with increase in heat input (figure 4a, 4b & 4c).

3.2 Tensile strength of weldment

The transverse tensile strength of all the joints made using different heat input conditions has been evaluated. In each condition three specimens were tested and the average tensile strength of three specimens per heat input and their corresponding percentage elongations thus obtained is mentioned in table 4. The tensile results so obtained show that maximum tensile strength of 640 MPa is possessed by the specimens made using low heat input combination followed by 605 MPa using medium heat input and 586 MPa using high heat input combination. The high tensile strength and ductility is possessed by the joints at low heat input, which can be attributed to smaller dendrite sizes and lesser inter-dendritic spacing in the fusion zone. Relatively lower tensile strength and ductility is possessed by the joints with long dendrite sizes and large inter-

dendritic spacing in the fusion zone of the joint welded using high heat input as shown in figure 7. Further it is found that all the tensile specimens fractured in the HAZ zone.

Table 4 Tensile test results

Heat input	Ultimate tensile strength (Mpa)	Elongation (%)
Low	640	28.771
Medium	605	24.450
High	586	20.083

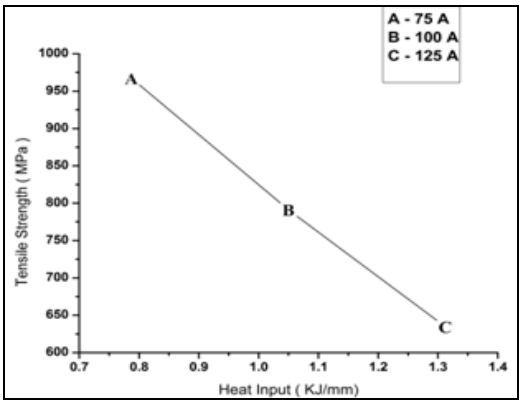

Fig.7 Tensile strength at different heat input

The fractured surfaces of the tensile specimens are shown figure 8a, 8b and 8c. Dimples of varying size and shape were observed in all the fractured surfaces. From figure 8a, it is observed that fractured surface of the specimen at low heat input contains a large population of small and shallow dimples which is indicative of its relatively high tensile strength and ductility. From figure 8b & 8c, it is observed that as heat input increases coarse and elongated dimples are observed. It is also observed that small dimples are surrounded by the large ones in all the specimens and a small quantity of tearing ridge is also present.

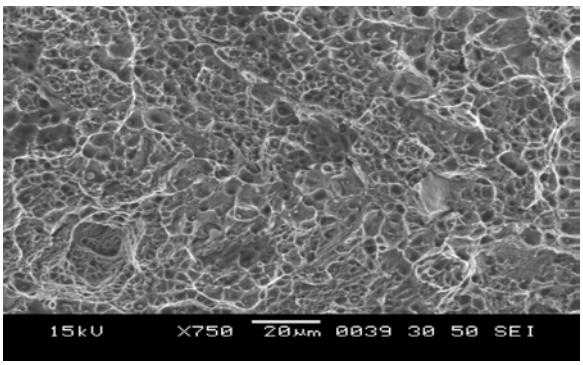

Fig.8 a) Dimple like structure shows ductile fracture at low heat input

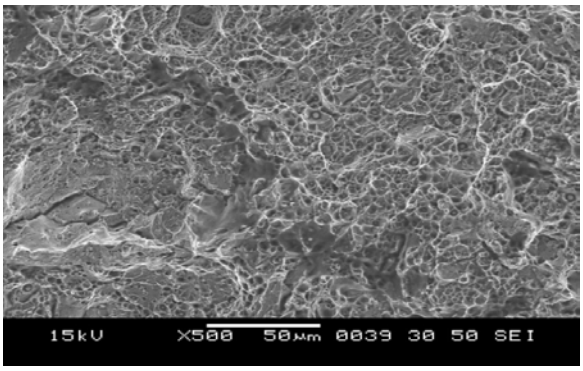

Fig.8 b) Partial brittle fracture at medium heat input

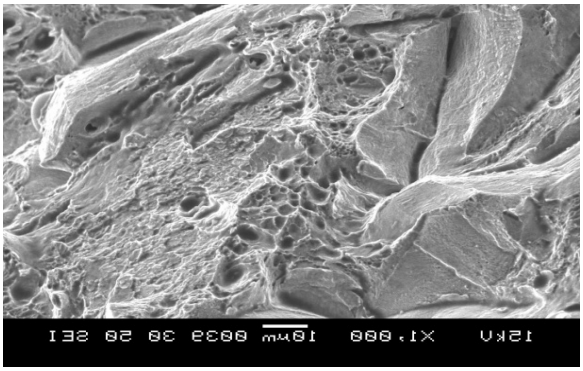

Fig.8 c) River like structure shows brittle fracture at high heat input

3.3.1 Effect of welding parameters on hardness of austenitic stainless steel

Tensile strength of austenitic stainless steel decreases with increase in welding parameters (welding current, voltage, and welding speed) because it is shown that during low heat input conditions width of HAZ is very small around the fusion zone which varies when changes to higher heat input. During higher heat input carbides precipitates a lot along the grain boundaries leading to sensitized zone around grain boundaries which helps in grain coarsening of HAZ zone and decrease in hardness around that area and finally the specimen undergoes brittle fracture at last under proper loading conditions. Micro-structural details of the weld metal in terms of dendrite size and cell spacing, indicates that high tensile strength and ductility is possessed by the joints at low heat input, which can be attributed to smaller dendrite sizes and lesser inter-dendritic spacing in the fusion zone. Relatively lower tensile strength and ductility is possessed by the joints with long dendrite sizes and large inter-dendritic spacing in the fusion zone of the joint welded using high heat input.

4 Conclusions

This study discusses the effect of heat input on tensile strength, micro-hardness and microstructure of austenitic 202 grade stainless steel weldments. Shielded metal arc welding was employed to weld the austenitic 202 grade stainless steel using 308L stainless steel solid electrode as the filler material. From the experimental results it was found that the increase in heat input affects the micro-constituents of base metal, and heat affected zone (HAZ). Experimental results showed that in fusion boundary there is a steep rise in the micro hardness with value of 218.7 VHN, 230.6 VHN and 258.4 VHN respectively for low, medium and high heat input respectively. In all the joints, HAZ area adjacent to the fusion boundary was coarse grained HAZ which possessed low hardness whereas the HAZ area adjacent to the base metal was fine grained HAZ which possessed high hardness. It is also observed that there is significant grain coarsening in the HAZs of all the joints. Further it is observed from the optical micrographs that the extent of grain coarsening in the HAZ increases with increase in heat input. Tensile strength of austenitic stainless steel decreases with increase in welding parameters because it is shown that during low heat input conditions width of HAZ is very small around the fusion zone which varies when changes to higher heat input. Micro-structural details of the weld metal in terms of dendrite size and cell spacing, indicates that high tensile strength and ductility is possessed by the joints at low heat input, which can be attributed to smaller dendrite sizes and lesser inter-dendritic spacing in the fusion zone. Relatively lower tensile strength and ductility is possessed by the joints with long dendrite sizes and large inter-dendritic spacing in the fusion zone of the joint welded using high heat input. Scanning electron microscopy showed that specimen fails due to ductile fracture at low heat input, specimen fails due to partial brittle fracture at medium heat input and specimen fails due to brittle fracture at high heat input.

References:

[1] A.J. Sedriks, Corrosion of stainless steel. 2nd edition. New York: Wiley; 1996.

[2] C.O.A Olsson, D. Landolt, Passive films on stainless steels-chemistry, structure and growth, Electrochimica Acta, Vol. 48(9), 2003, pp.1093-1104.

[3] D.M. Viano, N.U. Ahmed, G.O. Schumann, Influence of heat input and travel speed on microstructure and mechanical properties of double tandem submerged arc high strength low alloy steel weldments, Science and Technology of Welding & Joining, Vol.5(1), 2000, pp. 26-34.

[4] K. Prasad, D. K. Dwivedi , Some investigations on microstructure and mechanical properties of submerged arc welded HSLA steel joints, International Journal of Advanced Manufacturing Technology, Vol.36(5) , 2008, pp. 475-483.

[5] K. Prasad, D. K. Dwivedi, Microstructure and Tensile Properties of Submerged Arc Welded 1.25Cr-0.5Mo Steel Joints, Materials and Manufacturing Processes, Vol. 23(5), 2008, pp. 463-468.

[6] D.M. Viano, N.U. Ahmed, G.O. Schumann, Influence of heat input and travel speed on microstructure and mechanical properties of double tandem submerged arc high strength low alloy steel weldments, Journal of science and technology of welding and joining, Vol.5, 2000, pp. 26-34.

[7] G. Karthik, P. Karuppuswamy, V. Amarnath, Comparative Evaluation of Mechanical Properties and Micro Structural Characteristics of 304 Stainless Steel Weldments in TIG and SMAW Welding Processes, International Journal of Current Engineering and Technology, 2014, pp.200-206.

[8] P. Sathiya, S. Aravindan, P.M. Ajith, B. Arivazhagan, A. Noorul Haq, Microstructural characteristics on bead on plate welding of AISI 904 L super austenitic stainless steel using Gas metal arc welding process, International Journal of Engineering, Science and Technology, Vol. 2(6), 2010, pp. 189-199.

[9] D. Kianersi, A. Mostafaei, A. A. Amadeh, Resistance spot welding joints of AISI 316L austenitic stainless steel sheets: Phase transformations, mechanical properties and microstructure characterizations, Materials and Design 61, 2014, pp. 251–263.